

Astro2020 Science White Paper

The WFIRST Deep Grism Survey: WDGs

- Thematic Areas:**
- Planetary Systems
 - Star and Planet Formation
 - Formation and Evolution of Compact Objects
 - Cosmology and Fundamental Physics
 - Stars and Stellar Evolution
 - Resolved Stellar Populations and their Environments
 - Galaxy Evolution
 - Multi-Messenger Astronomy and Astrophysics

Principal Author:

Name: R. E. Ryan

Institution: Space Telescope Science Institute (STScI)

Email: rryan@stsci.edu

Phone: (410) 338-4352

Co-authors:

S. Malhotra (GSFC)	N. Pirzkal (STScI)	S. L. Finkelstein (UT)	R. L. Larson (UT)
J. E. Rhoads (GSFC)	N. P. Hathi (STScI)	R. A. Jansen (ASU)	R. A. Lucas (STScI)
A. Koekemoer (STScI)	I. G. B. Wold (GSFC)	P. Nair (UA)	B. Joshi (ASU)
M. Bradač (UC, Davis)	R. A. Windhorst (ASU)	N. A. Grogin (STScI)	

Abstract

The Wide-Field Infrared Survey Telescope (WFIRST) is a planned 2.4-m space telescope with a suite of broadband filters and two slitless spectroscopic modes that cover an instantaneous field-of-view of $\sim 0.28 \text{ deg}^2$ at wavelengths from $\sim 0.6 - 2.0 \mu\text{m}$. One core program for WFIRST is the High-Latitude Survey (HLS), which plans to obtain broadband imaging over $\sim 2200 \text{ deg}^2$ with slitless spectroscopy to a line flux sensitivity of $10^{-16} \text{ erg s}^{-1} \text{ cm}^{-2}$ and measure spectroscopic redshifts accurate to $\sigma_z/(1+z) \lesssim 0.1\%$. Although this survey will be instrumental in advancing a vast array of scientific topics from cosmology to Galactic stellar populations, we identify several open questions that require dedicated deep observations. Here we focus on the need for a WFIRST Deep Grism Survey (WDGS) that WFIRST would uniquely enable. We expect the WDGs should reach a line-flux sensitivity of at least $5 \times 10^{-18} \text{ erg s}^{-1} \text{ cm}^{-2}$, observe multiple position angles, and cover $\sim 0.6 \text{ deg}^2$, which would require an exposure time of $\gtrsim 100 \text{ hr}$. Additionally, the WDGs would buttress the HLS by providing a self-consistent set of contamination-corrected spectra, sample purity, and extended-source redshift accuracy.

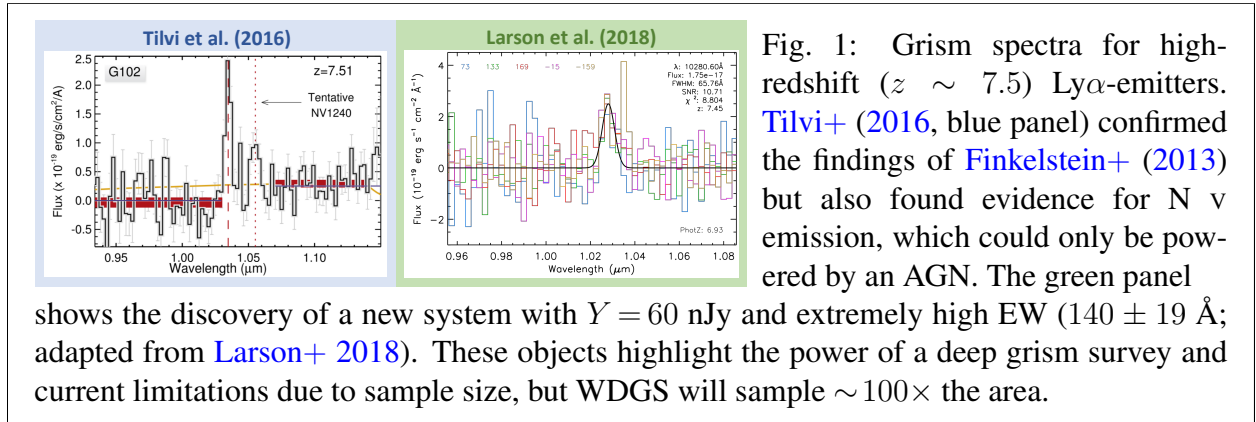
The combination of near-infrared spectroscopy and deep optical imaging is the unrivaled dataset for studying the physical properties of galaxies (such as star formation, metallicity, and dust extinction) at the peak of the cosmic star-formation rate density ($1 \lesssim z \lesssim 2$). Therefore, it would be highly desirable to place this deep field in a region of comparably deep panchromatic imaging, such as that provided by the Large Synoptic Survey Telescope (LSST).

1 Key Science Questions

We discuss several open scientific questions that will not be resolved by the WFIRST High-Latitude Survey (HLS; [Spergel+ 2015](#)) and that demand a concerted effort from a deep grism survey. To set the stage, we define the WFIRST Deep Grism Survey (WDGS) as having:

1. **Multiple position angles (PAs):** Overlapping traces of neighboring sources significantly limit the fidelity of slitless spectroscopy, but multiple PAs provide a self-consistent model for any scene, mitigate contamination, and improve spectral resolution ([Ryan+ 2018](#)).
2. **Mosaicked pointing:** The aspect ratio of the Wide-Field Imager (WFI; 1:2) is not conducive to surveying a large area with multiple PAs, particularly if they are separated by $\gtrsim 10^\circ$. Therefore we consider a 2×1 mosaic with the WFI, which is nominally $\sim 0.6 \text{ deg}^2$;
3. **Long exposure time:** Based on observations with HST/WFC3 (e.g. [Pirzkal+ 2017](#)), we expect to reach a line sensitivity $(5 - 10) \times 10^{-18} \text{ erg s}^{-1} \text{ cm}^{-2}$ in the equivalent of 60 HST orbits ($\sim 40 - 50 \text{ hr}$). Therefore in the 2×1 mosaic, WDGS would need $\sim 100 \text{ hr}$.

1.1 The Five W's of Cosmic Reionization: Who, What, When, Where, Why? — The measurements of the Ly α emission line from galaxies has not only been the primary method for confirming the redshifts of galaxies at $z > 3$ (e.g. [Finkelstein 2016](#)), but also has the potential to place stringent constraints on the evolution of the reionization of the intergalactic medium (IGM; [Miralda-Escudé 1998](#); [Malhotra & Rhoads 2004](#); [Dijkstra 2014](#)). As this line is resonantly scattered by neutral hydrogen, star-forming galaxies can act as Ly α lighthouses, visible from ionized epochs, but attenuated by the fog of H I during neutral epochs. Fortunately, the physical processes at play in galaxies (likely reduced dust attenuation and a lower H I column density) conspire to promote the escape of Ly α from galaxies, with $\sim 50\%$ of spectroscopically observed galaxies at $z \sim 6$ showing significant Ly α emission with modest equivalent widths ($\text{EW} > 25 \text{ \AA}$; [Stark+ 2010, 2011](#)). Thus, star-forming galaxies at $z > 6$ are useful tools for measuring the evolution of the IGM, even as it becomes more neutral and the Ly α detection rate decreases.



Significant observational effort has gone into the search for Ly α emission at $z > 6.5$, with the consensus being that the Ly α EW distribution is evolving to lower values at higher redshifts, consistent with what is expected for an evolving IGM neutral fraction (e.g. [Fontana+ 2010](#); [Pentericci+ 2014](#); [Mason+ 2018](#); [Jung+ 2018](#)). Since these observations are predominantly from large ground-based telescopes, they suffer from several sources of incompleteness: wavelength coverage, sensitivity, and night sky emission lines. While these effects can be modeled, they limit the sample sizes and inferences of the evolution of reionization.

While extremely-large ground-based telescopes will represent a tremendous advance in our spectroscopic sensitivity, they lose $\sim 50\%$ of their wavelength coverage due to telluric emission. Spectroscopic surveys from space represent an attractive alternative to complement the ground-based facilities. Thanks to significantly lower backgrounds, space-based surveys can effectively implement slitless spectroscopy, which simultaneously increases the redshift-discovery space and removes many selection biases (such as target selection or fiber/slit density). The Faint Infrared Grism Survey (FIGS; Pirzkal+ 2017) is a large HST/WFC3 program targeting putative high redshift galaxies ($6 < z < 8$) in four fields. With a limiting sensitivity of 10^{-17} erg s $^{-1}$ cm $^{-2}$, FIGS detected two Ly α emission lines at $z > 7$ (Tilvi+ 2016; Larson+ 2018, see Fig. 1). Based on published luminosity functions (Finkelstein 2016) and EW distributions (Wold+ 2017), we expect that WDGS should detect $\gtrsim 2000$ Ly α emitters at $z > 7.2$.

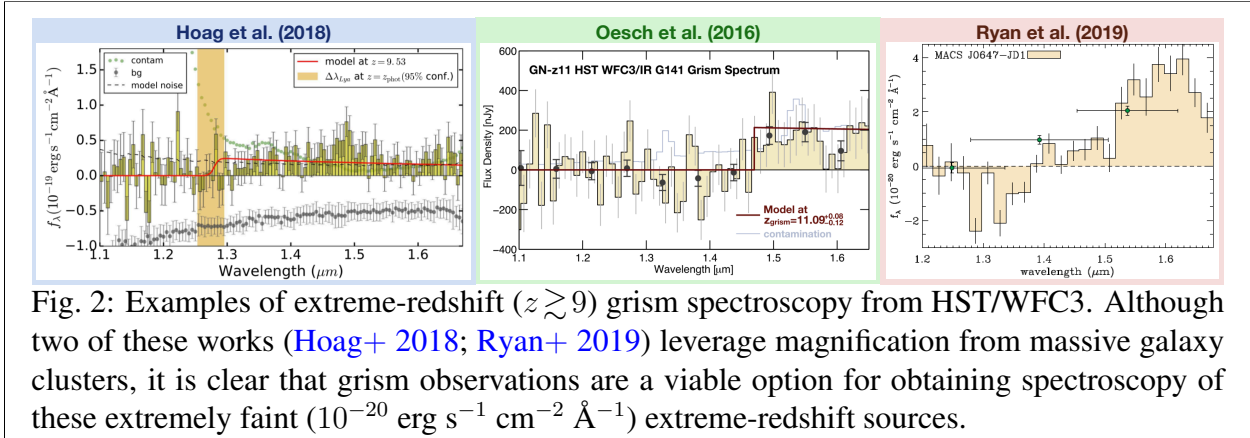


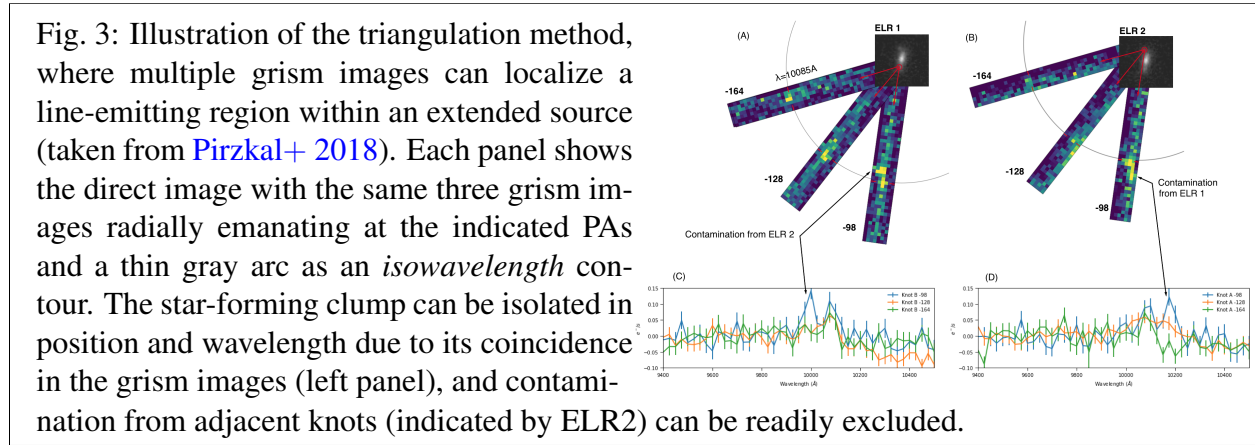
Fig. 2: Examples of extreme-redshift ($z \gtrsim 9$) grism spectroscopy from HST/WFC3. Although two of these works (Hoag+ 2018; Ryan+ 2019) leverage magnification from massive galaxy clusters, it is clear that grism observations are a viable option for obtaining spectroscopy of these extremely faint (10^{-20} erg s $^{-1}$ cm $^{-2}$ Å $^{-1}$) extreme-redshift sources.

The WDGS will also have the sensitivity to probe the extreme-redshift regime ($z \gtrsim 9$) by means of detecting the neutral hydrogen absorption at $\lambda_{\text{rest}} \leq 1216$ Å (*e.g.* Gunn & Peterson 1965). To date, Ly α -breaks have been conclusively identified in at least three systems at these redshifts (see Fig. 2) using less exposure time than considered here. Although these objects lack Ly α emission, they are still relatively direct probes of the cosmic ultraviolet luminosity density and place important constraints on the evolution of reionization (*e.g.* Robertson+ 2015; Bouwens+ 2015; Finkelstein 2019). Analysis of the grism spectroscopy and broadband photometry suggests that these galaxies typically formed $\sim 100 - 200$ Myr after the Big Bang (Hoag+ 2018; Oesch+ 2016; Ryan+ 2019), which implies a significant burst of star-formation prior to the assembly of the dark matter halo (*e.g.* Trenti+ 2015). However unlikely this might seem, it is premature to say if this tension is real or an artifact of the analysis (such as strong emission lines affecting the optical colors; de Barros+ 2014; Smit+ 2014) with so few spectroscopically-confirmed objects. These sparse samples lead to vastly different inferred luminosity densities (*e.g.* Coe+ 2013; Oesch+ 2014; Bouwens+ 2016; Oesch+ 2018), but WDGS should find $\gtrsim 20$ sources at $z \gtrsim 9$ based on the samples found in the pure-parallel programs (Bernard+ 2016; Morishita+ 2018).

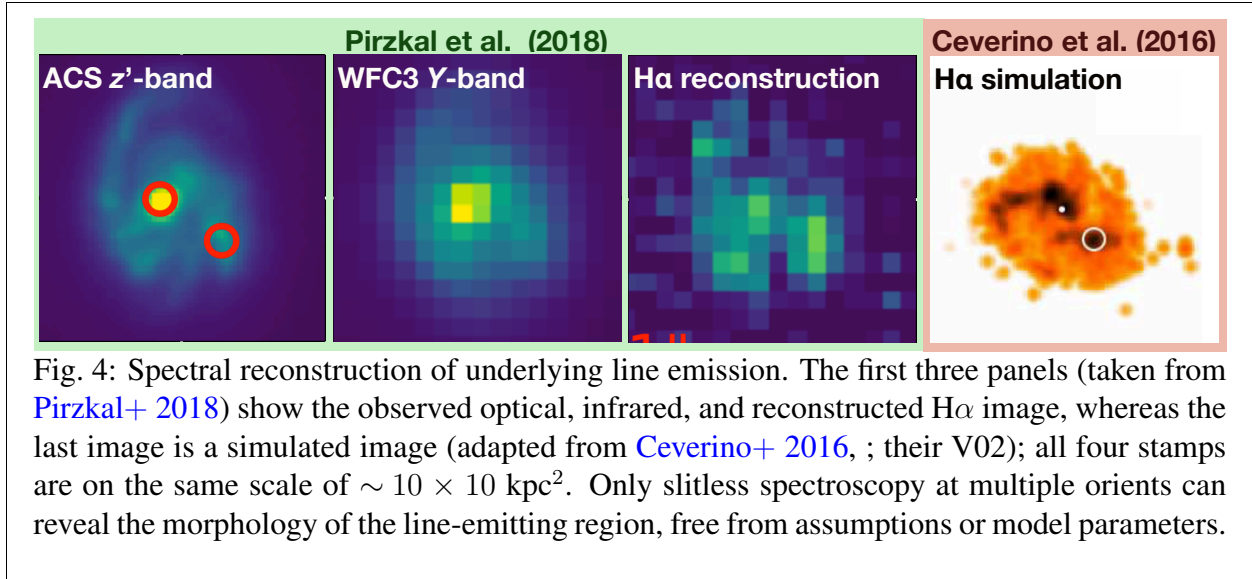
1.2 How does Star Formation Progress and Quench in Disk Galaxies? — Massive disk galaxies ($M_{\star} \sim 10^{10} M_{\odot}$) often exhibit clumpy morphologies (*e.g.* Elmegreen & Elmegreen 2005), however the nature and fate of these clumps, and the role that they play in the evolution of their host galaxies is under significant debate. From a theoretical standpoint, the clumps form from minor merging and “violent” disk instabilities (*e.g.* Dekel+ 2009a,b), and the lowest mass clumps dissolve in a few free-fall times (*e.g.* Ceverino+ 2016; Mandelker+ 2017). But since the

infalling gas is generally of lower metallicity (than that of the host), they are expected to show strong age and metallicity gradients, which is broadly consistent with observations (*e.g.* Soto+ 2017). Conversely, the densest, most massive clumps likely coalesce in the center of the host, forming the present-day bulges (*e.g.* Elmegreen+ 2008; Ceverino+ 2010; Nataf 2017).

Since these clumps are generally very small ($\lesssim 1$ kpc), their study demands space-based resolution, and wide-field HST imaging (*e.g.* Koekemoer+ 2011; Grogin+ 2011; Rafelski+ 2015) has been instrumental in advancing the field. For example, only recently have large statistical samples, constructed based on algorithmic definitions, been possible (*e.g.* Guo+ 2012, 2015, 2018), and their demographics are broadly consistent with the minor-merging and violent disk instability evolutionary scenarios: the clumps often contribute little to the UV flux, but represent a minority of the star-formation (Guo+ 2015; Soto+ 2017).



However moving from sample demographics to physical understanding requires spectroscopy, which is exceedingly challenging to obtain on these spatial and brightness scales. To this end, our team has pioneered techniques to use slitless spectroscopy at multiple PAs to extract spectra of the clumps (see Fig. 3 for an illustrative example), and improve the understanding of their star-formation processes. The clumps are generally strong line-emitters (Straughn+ 2008), with rest-frame $EW \gtrsim 100 \text{ \AA}$, but their line-luminosity functions (of $H\alpha$, $[O \text{ III}]$, and $[O \text{ II}]$) evolve considerably with redshift (Pirzkal+ 2013). Like Soto+ (2017), we have shown that these clumps are rarely centrally located (Pirzkal+ 2013), with $\sim 44\%$ of the clumps beyond one half-light radius (Pirzkal+ 2018). In addition to facilitating the study of the star-forming clumps, it also foreshadows a source for concern in emission-line redshifts from slitless spectroscopy of resolved sources: The observed wavelength of the emission line depends on the position of the line-emitting region, which is generally displaced from the barycenter of the host object (see Fig. 3). If unaccounted for, this displacement leads to a shift in observed wavelength, hence a random offset in the inferred redshift, which based on the typical properties of $z \sim 1$ galaxies is $\sigma_z/(1+z) \sim 0.07\%$ (Ryan+ 2016). As this is approaching the redshift tolerance specified by Spergel+ (2015), a deep, multi-orient grism survey will pay dividends in calibrating the spectroscopic redshifts of the entire mission.



The triangulation philosophy can be extended to provide a complete reconstruction of the underlying, two-dimensional profile of the line-emission (Pirzkal+ 2018, see Fig. 4 for an example of an H α realization for a galaxy at $z=0.42$). Similarly, Hviding+ (2018) expand on our techniques to identify 8 galaxies at $z\sim 0.9$ that have extended low-ionization emission regions (LIERs — in contrast to the classic definition of LINERs; Heckman 1980). The Pirzkal+ (2018) and Hviding+ (2018) works are the first measurements approaching the peak of the cosmic star-formation rate density that are directly comparable with the simulations (*e.g.* Ceverino+ 2016), which show that the rapid accretion of low-metallicity gas fuels strong H α emission in a clumpy disk (see fourth panel in Fig. 4). Pirzkal+ (2018) find that $\sim 40\%$ ($= 38/153$) of H α sources in ~ 18 arcmin² that show extended emission like Fig. 4, suggesting WDGS should find $\sim 6,000$ such sources and move from sample demographics to sample physics. Since this reconstruction is limited by the signal-to-noise at a given PA, the HLS will provide little in examining the two-dimensional morphology of the line-emitting gas unlike the WDGS.

1.3 How to Study the Most Extreme Emission-Line Galaxies? — The most powerful aspect of slitless spectroscopy is that it provides a complete multiplexing without imposing any observer-based biases. Perhaps the most dramatic example of which comes from the study of extreme-emission line galaxies (EELGs), which are systems with a weak continuum and strong emission lines (with $EW \gtrsim 500$ Å in the most extreme cases; Atek+ 2012). These galaxies have low dynamical masses, high specific star-formation rates, and compact sizes (*e.g.* van der Wel+ 2011; Maseda+ 2013), often leading to a self-regulatory surface brightness limit (Meurer+ 1997). Although ground-based telescopes have the sensitivity to detect their emission lines, the EELGs are largely unobserved since they fail to make brightness selection criteria. Since slitless spectroscopy is much less affected by this bias, these sources are easily detected in shallow surveys (van der Wel+ 2011), which have shown that these galaxies sit off the star-formation main sequence (Finkelstein+ 2015) and mass-metallicity relationship (Pharo+ 2018). In cases of high [O III]/[O II] ratios, these galaxies also exhibit very large Lyman continuum flux, with escape fractions that reach $\sim 70\%$ (Izotov+ 2018)!

The Sloan Digital Sky Survey (SDSS) has been instrumental in identifying and characterizing the EELGs (colloquially called *green peas* based on their compact, green appearance in SDSS

imaging; Cardamone+ 2009). WDGs will extend the discovery space for EELGs/green peas to $z \sim 2$ into the epoch of peak star-formation rate density, probing 10^7 Mpc^3 , and allow a study of the evolution of their number counts. Based on the SDSS results, WDGs should identify $\gtrsim 20$ high-redshift EELGs.

1.4 What about the Halo and Thick-Disk Brown Dwarfs? — Since brown dwarfs do not fuse hydrogen in their cores, they are constantly cooling throughout their lifetimes and so can serve as chronometers to examine the star-formation history of the Milky Way. For example, an instantaneous burst of star formation at very early times will result in a Galactic thin disk that has no warm brown dwarfs ($\sim L0$), as they have cooled to lower spectral types ($\sim T0$). This results in a disk with an increased number of ultracool dwarfs ($\sim T0$) with respect to the initial mass function (Burgasser 2004). Similarly, Ryan+ (2017) showed that thickness of the disk of brown dwarfs will vary with spectral type, such that spectral types below the hydrogen-burning limit will populate a disk thinner than that of stars on the end of the main sequence. The depth of this deviation will increase with the ratio of recent-to-old star formation, and so the number counts of brown dwarfs can be used to mine the fossil record of the Milky Way.

The number and properties of brown dwarfs in the Galactic thick disk and halo are powerful constraints on the cooling models (*e.g.* Burrows+ 2001; Baraffe+ 2003; Saumon & Marley 2008) and/or the Galactic star-formation history. While the HLS will be indispensable for studying the stellar populations of the Milky Way, it lacks the depth to reach brown dwarfs in the thick disk or Galactic halo. Ryan & Reid (2016) predict that a deep field at high Galactic latitude should expect ~ 100 brown dwarfs, which would sample the substellar portion of these older Galactic components in a modest area for the first time.

2 Value Added by the WDGs

The HLS has several goals, some of which require reasonably precise redshifts ($\sigma_z/(1+z) \sim 0.1 - 0.5\%$; Spergel+ 2015) with a well understood completeness. A deep grism survey like WDGs represents the only way to empirically assess the completeness of the HLS by comparing the properties of the detected sources. For example, the primary HLS imaging and spectroscopy are likely to be rather shallow (7σ line flux sensitivity of $10^{-16} \text{ erg s}^{-1} \text{ cm}^{-2}$; Spergel+ 2015), allowing extreme-emission line galaxies to go undetected in the direct image(s). A deep spectroscopic campaign can identify the prevalence of unexpected systems, which can be included in the completeness calculations for the HLS.

3 Deep Spectroscopy in the 2020s

The astronomical landscape of the 2020s will be marked by the emergence of large surveys, telescopes, and instruments, but the WDGs will occupy a unique part of parameter space not accessible by planned missions. In many respects, WFIRST and Euclid are symbiotic missions: they are focused on wide area optical/infrared imaging and grism spectroscopy. However, the similarities end there: with its smaller aperture and larger pixel scale, the Euclid spectroscopy will be of lower quality than that of WFIRST. Nevertheless, Euclid will be an important pathfinder to the wide-field spectroscopy we can expect with WFIRST. Additionally, the Prime Focus Spectrograph (PFS) on Subaru will cover 1.2 deg^2 with ~ 2000 fibers and reach impressive depths for $\lambda \lesssim 1.2 \mu\text{m}$. PFS will be subject, however, to the usual concerns with a fiber-fed spectrograph from the ground (source selection, fiber size and packing, sky emission, *etc.*), *leaving WDGs as the only option for deep, unbiased spectroscopy at $\gtrsim 1 \mu\text{m}$.*

References

- Atek, H., et al. 2011, *ApJ*, 743, 121
- Bacon, R., et al. 2017, *A&A*, 608, 20
- Baraffe, I., Chabrier, G., Barman, T. S., Allard, F. & Hauschildt, P. H. 2003, *A&A*, 402, 701
- Bernard, S. R., et al. 2016, *ApJ*, 827, 76
- Bouwens, R. J., et al. 2015, *ApJ*, 811, 140
- Bouwens, R. J., et al. 2016, *ApJ*, 830, 67
- Burgasser, A. J., 2004, *ApJS*, 155, 191
- Burrows, A., Hubbard, W. B., Lunine, J. I., & Liebert, J. 2001, *RvMP*, 73, 719
- Cardamone, C., et al. 2009, *MNRAS*, 399, 1191
- Ceverino, D., Dekel, A., & Bournaud, F. 2010, *MNRAS*, 404, 2151
- Ceverino, D., et al. 2016, *MNRAS*, 457, 2605
- Coe, D., et al. 2013 *ApJ*, 762, 32
- de Barros, S., Schaerer, D., & Stark, D. P. 2014, *A&A*, 563, A81
- Dekel, A., Sari, R., & Ceverino, D. 2009, *ApJ*, 703, 785
- Dekel, A., et al. 2009, *Natur*, 457, 451
- Dijkstra, M., 2014, *PASA*, 31, 40
- Elmegreen, B. G. & Elmegreen, D. M. 2005, *ApJ*, 627, 632
- Elmegreen, B., G., Bournaud, F., & Elmegreen, D. M. 2008, *ApJ*, 688, 67
- Finkelstein, S. L., et al. 2013, *Natur*, 502, 524
- Finkelstein, K. D., et al. 2015, *ApJ*, 813, 78
- Finkelstein, S. L., 2016, *PASA*, 33, 37
- Finkelstein, S. L., et al. 2019, *ApJ*, submitted, arXiv: 1902.02792
- Fontana, A., et al. 2010, *ApJL*, 725, L205
- Grogin, N. A., 2011, *ApJS*, 197, 35
- Gunn, J. E., & Peterson, B. A. 1965, *ApJ*, 142, 1633
- Guo, Y., et al. 2012, *ApJ*, 757, 120
- Guo, Y., et al. 2015, *ApJ*, 800, 39
- Guo, Y., et al. 2018, *ApJ*, 853, 108
- Hoag, A., et al. 2018, *ApJ*, 854, 39
- Heckman, T. M., 1980, *A&A*, 87, 152
- Hviding, R., et al. 2018, *ApJ*, 868, 16
- Izotov, Y. I., et al. 2018, *MNRAS*, 478, 4851
- Jung, I., et al. 2018, *ApJ*, 864, 103
- Jung, I., et al. 2019, *ApJ*, in prep
- Koekemoer, A. M., 2011, *ApJS*, 197, 36
- Larson, R. L., et al. 2018, *ApJ*, 858, 94

Lotz, J. M., et al. 2017, ApJ, 837, 97
Malhotra, S. & Rhoads, J., 2004, ApJ, 617, 5
Mandelker, N. et al. 2017, MNRAS, 464, 635
Maseda, M. V., et al. 2013, ApJL, 778, 22
Mason, C., et al. 2018, ApJ, 857, 11
Meurer, G., et al. 1997, AJ, 114, 54
Miralda-Escudé, J., 1998, ApJ, 501, 15
Morishita, T., et al. 2018, ApJ, 867, 150
Nataf, D. M. 2017, PASA, 34, 41
Oesch, P. A., et al. 2014, ApJ, 786, 108
Oesch, P. A., et al. 2016, ApJ, 819, 129
Oesch, P. A., et al. 2018, ApJ, 855, 105
Pentericci, L., et al. 2014, ApJ, 793, 113
Pharo, J., et al. 2018, ApJ, accepted, arXiv: 1810.12342
Pirzkal, N. et al. 2013, ApJ, 772, 48
Pirzkal, N., et al. 2015, ApJ, 804, 11
Pirzkal, N., et al. 2017, ApJ, 846, 84
Pirzkal, N., et al. 2018, ApJ, 868, 61
Postman, M., et al. 2012, ApJ, 756, 159
Rafelski, M., et al. 2015, AJ, 150, 31
Robertson, B., et al. 2015, ApJL, 802, 19R
Ryan, R. E. & Reid, I. N., 2016, AJ, 151, 92
Ryan, R. E., Casertano, S., & Pirzkal, N. 2016, WFIRST-TIR, 1606
Ryan, R. E., et al. 2017, ApJ, 847, 53
Ryan, R. E., Casertano, & Pirzkal 2018, PASP, 985, 034501
Ryan, R. E., et al. 2019, ApJL, in prep
Saumon, D., Marley, M. S. 2008 ApJ, 689, 1327
Smit, R., et al. 2014, ApJ, 784, 58
Soto, E., et al. 2017, ApJ, 837, 6
Spergel, D. N., et al. 2013, arXiv: 1503.03757
Stark, D. P., et al. 2010, MNRAS, 408, 1628
Stark, D. P., et al. 2011, ApJ, 728, 2
Straughn, A. N., 2008, AJ, 135, 1624
Tilvi, V., et al. 2016, ApJL, 827, 14
Trenti, M., Perna, R., & Jimenez, R. 2015, ApJ, 802, 103
van der Wel, A. et al. 2011, ApJ, 742, 111
Wold, I. G. B., et al. 2017, ApJ, 848, 108